Thermodynamic properties of ferrimagnetic spin chains in the presence of a magnetic field

J. Abouie,[1] S. A. Ghasemi,[1,2] and A. Langari[1,3]
[1]*Institute for Advanced Studies in Basic Sciences, Zanjan 45195-1159, Iran*
[2]*Institut für Physik, Universität Basel, Basel, Switzerland*
[3]*Physics Department, Sharif University of Technology, Tehran 11365-9161, Iran*
(Received 17 August 2005; revised manuscript received 24 October 2005; published 17 January 2006)

We have implemented three approaches to describe the thermodynamic properties of ferrimagnetic ($S=5/2$, $s=2$) spin chains. The application of cumulant expansion has been generalized to the ferrimagnetic chain in the presence of an external magnetic field. Using cumulants, we have obtained the field-dependent effective Hamiltonian in terms of the classical variables up to the second order of quantum corrections. Thermodynamic functions, the internal energy, the specific heat, and the magnetic susceptibility are obtained from the effective Hamiltonian. We have also examined the modified spin-wave theory to derive the same physical properties. Finally, we have studied our model using quantum Monte Carlo simulation to obtain accurate results. The comparison of the above results and also the high temperature series expansion shows that cumulant expansion gives good results for moderate and high temperature regions while the modified spin wave theory is good for low temperatures. Moreover, the convergence regions of the cumulant expansion and the modified spin-wave theory overlap each other which propose these two as a set of complement methods to get the thermodynamic properties of spin models.

DOI: 10.1103/PhysRevB.73.014411 PACS number(s): 75.40.−s, 75.10.Hk, 75.10.Jm

I. INTRODUCTION

It will become evident that there are numerous highly interesting experimental systems which are effectively one-dimensional (1D) models. The 1D models are more interesting from the theoretical point of view. The quantum effects which are highlighted in the 1D spin models represent alternative physical behavior. In this class, quantum ferrimagnets are mixed spin systems with antiferromagnetic interactions. Mostly, they are composed of the two type of spins, $S \neq s$. Two families of ferrimagnetic chains are described by $A\mathrm{Cu}(pba)(\mathrm{H_2O})_3 \cdot n\mathrm{H_2O}$ and $A\mathrm{Cu}(pbaOH)(\mathrm{H_2O})_3 \cdot n\mathrm{H_2O}$, where *pba*=1,3-*propylenebis*(*Oxamato*), *pbaOH*=2-*hydroxo*-1,3-*propylenebis*(*Oxamato*) and *A*=Ni, Fe, Co, and Mn.[1–3] Ferrimagnets, which occur rather frequently in nature, are somehow between the antiferromagnets and the ferromagnets. Despite the fact that the homogeneous integer spin chains show the Haldane gap in their low energy spectrum and the half-integer ones are gapless,[4] 1D ferrimagnets behave differently. The lowest energy band of the 1D ferrimagnets is gapless which shows a ferromagnetic behavior while there is a finite gap to the next band above it which has the antiferromagnetic properties.[5–7] It is the acoustical and optical nature of excitations which is the result of two different type of spins in each unit cell. This behavior has been observed in the low and high temperature regime of quantum ferrimagnets.[6] There are many approaches to study the properties of the ferrimagnetic chains; The dual features of ferrimagnetic excitations can be illuminated by using the density-matrix renormalization group (DMRG)[5,8] and quantum Monte Carlo (QMC) methods.[7,9] Numerical diagonalization, combined with Lanczos algorithm[10] and the scaling technique,[11] further have been applied to study the modern topics such as the phase transition[10,12] and the quantized magnetization plateau.

The discovery of both ferromagnetic gapless and antiferromagnetic gapped excitations have led to the investigation of the thermodynamic properties. It has been predicted that the specific heat at high temperatures should behave like an antiferromagnet[6] that exhibits a Schottky peak at the intermediate temperatures. The modified spin-wave theory (MSWT) and QMC can be used to see this behavior; however, QMC is not able to reach low temperatures sufficiently to completely demonstrate the ferromagnetic behavior.[6]

Most of the mentioned techniques such as QMC and DMRG have been used for ferrimagnets with small spins. The Hilbert space of large spins are growing exponentially and make the computations more difficult. In recent years there have been considerable attempts which have focused on the properties of new magnetic materials, such as magnetic molecules with large effective spins (S,s), or intermetallic compounds containing magnetic layers or chains. Using MSWT[13] and high temperature series expansion (HTSE),[14] one can describe the low temperature and high temperature properties of these systems, respectively. Moreover, the HTSE is not accurate enough, even by taking into account higher terms (11th and 7th terms for specific heat and susceptibility, respectively). In addition the validity regime of HTSE is too far from the low temperature regime of MSWT to cover the full range of temperature. The midtemperature behavior of ferrimagnets with large values of S and s, has not received sufficient attention. In this respect, we used the MSWT to describe the thermodynamic behavior of the ferrimagnetic large spin chains. We have also implemented the QMC simulation[15] as an accurate result for comparison. At moderate temperatures, i.e, $Js < T < JSs$ (J is the exchange coupling) the results of MSWT do not coincide with QMC ones. Therefore, to describe the physical properties at midtemperatures we have employed the cumulant expansion (CE).[16,17] Recently, this method has been used to

study the finite temperature behavior of large spin ferromagnetic and antiferromagnetic systems.[18–21]

In this article we have generalized the application of CE to obtain the magnetization and magnetic susceptibility of ferrimagnets. Moreover, the QMC simulation for the ($S=5/2$, $s=2$) ferrimagnetic chain has been done to see the accurate behavior. We have observed good agreement between the QMC and CE results in the intermediate and high temperature regions. The outline of this paper is as follows: In Sec. II we have employed three theoretical approaches: CE, QMC simulation, and MSWT. The effective Hamiltonian and magnetization in the presence of the magnetic field are obtained using the CE up to the second order of $(\beta\tilde{J}/s)$. In Sec. III the results and discussions are demonstrated. We have compared our approaches with the high temperature series expansion (HTSE). It has been observed that CE and MSWT are two complementary methods to get a good description of large spin ferrimagnetic chains for the whole range of temperatures.

II. THEORETICAL APPROACHES

A. Cumulant expansion

Thermodynamic functions of any quantum spin system with a Hamiltonian $\hat{H}$ can be obtained by differentiation of the quantum partition function ($\mathcal{Z}$) or its logarithm with respect to the appropriate parameters. Using the basis of spin-coherent states $|\{\mathbf{n}_i\}\rangle$,[22] the trace of an operator is reduced to the integral over a set of classical vectors, so the partition function is reduced to that of an effective classical spin system with the Hamilton function $\mathcal{H}$.[18–21] The effective Hamiltonian $\mathcal{H}$ can be expanded in terms of cumulants[16,17] of the powers of $\hat{H}$ as follows:

$$\beta\mathcal{H} = \beta\langle\hat{H}\rangle^c - \frac{\beta^2}{2!}\langle\hat{H}\hat{H}\rangle^c + \frac{\beta^3}{3!}\langle\hat{H}\hat{H}\hat{H}\rangle^c + \cdots = \beta(\mathcal{H}^{(0)} + \mathcal{H}^{(1)} + \mathcal{H}^{(2)} + \cdots), \quad (1)$$

where $\beta=1/T$ and $\langle O\rangle^c$ represents the cumulant of operator O.[16,17] The function $\mathcal{H}$ evidently depends on the temperature, thus the calculation of the physical quantities should be done with care.

Let us consider the Hamiltonian ($\hat{H}$) of a ferrimagnetic chain which is composed of two kinds of spins, S and s ($S>s$), alternatively,

$$\hat{H} = \sum_{i,j}^{N/2,N/2} J_{2i-1,2j}\mathbf{S}_{2i-1}\cdot\mathbf{s}_{2j} - \sum_{i}^{N/2}\mathbf{H}_{2i-1}\cdot\mathbf{S}_{2i-1} - \sum_{i}^{N/2}\mathbf{H}_{2i}\cdot\mathbf{s}_{2i}, \quad (2)$$

where $\mathbf{H}_i$'s are the external magnetic field at each sites. Expressing the spin operator on each site in the coordinate system with the z axis along the coherent state vector $\mathbf{n}_i^z=\mathbf{n}_i$

$$\mathcal{H} = \mathcal{H}^{(0)} + \mathcal{H}^{(1)} + \mathcal{H}^{(2)} + \mathcal{H}_h^{(0)} + \mathcal{H}_h^{(1)} + \mathcal{H}_h^{(2)}, \quad (3)$$

where $\mathcal{H}^{(0)}$ is the pure classical contribution, and $\mathcal{H}^{(1)}$ and $\mathcal{H}^{(2)}$ are the quantum corrections in the absence of a magnetic field (see Refs. 20 and 21). The field-dependent terms $\mathcal{H}_h^{(i)}$ will be expressed in the following forms:

$$\mathcal{H}_h^{(0)} = -\omega\sum_{i}^{N/2}\mathbf{h}_{2i-1}\cdot\mathbf{n}_{2i-1} - \sum_{i}^{N/2}\mathbf{h}_{2i}\cdot\mathbf{n}_{2i},$$

$$\mathcal{H}_h^{(1)} = \frac{\beta\omega}{2s}\sum_{i,j}^{N/2,N/2}\tilde{J}_{2i-1,2j}[(\mathbf{h}_{2i-1}\cdot\mathbf{n}_{2j}) - (\mathbf{h}_{2i-1}\cdot\mathbf{n}_{2i-1}) \times(\mathbf{n}_{2i-1}\cdot\mathbf{n}_{2j}) + (\mathbf{h}_{2j}\cdot\mathbf{n}_{2i-1}) - (\mathbf{h}_{2j}\cdot\mathbf{n}_{2j})(\mathbf{n}_{2i-1}\cdot\mathbf{n}_{2j})] - \frac{\beta}{4s}\sum_{i}[\omega(1-(\mathbf{h}_{2i-1}\cdot\mathbf{n}_{2i-1})^2) + 1 - (\mathbf{h}_{2i}\cdot\mathbf{n}_{2i})^2], \quad (4)$$

where $\omega=S/s$. In the above expressions $\tilde{J}=Js^2$ and $\mathbf{h}=\mathbf{H}'s$ are the exchange interaction and the reduced magnetic field, respectively. Again, $\mathcal{H}_h^{(0)}$ is the classical contribution and the remaining higher orders are responsible for quantum corrections. The field-dependent terms of order h^3, Jh^2, and hJ^2 in $\mathcal{H}_h^{(2)}$ can be calculated with the help of cumulants corresponding to the mixed field-exchange terms. These terms are too lengthy and have been presented in the appendix. Quasiclassical expansion up to second order of $[O(1/s^2)]$ for the internal energy and the specific heat were investigated for different S, s in Refs. 20 and 21. We will now calculate the CE of the magnetization and the susceptibility. In order to get the physical concept we have considered the nearest neighbor interaction and that the applied fields on each site are in the same direction, i.e., $\mathbf{h}_i=h\mathbf{n}$. Thus, the field-dependent terms of the effective Hamiltonian are reduced to the following forms:

$$\mathcal{H}_h^{(0)} = -h\mathbf{n}\cdot\sum_{i=1}^{N/2}(\mathbf{n}_{2i} + \omega\mathbf{n}_{2i-1}),$$

$$\mathcal{H}_h^{(1)} = \frac{\beta h\omega\tilde{J}}{2s}\sum_{i=1}^{N}\{2\mathbf{n}\cdot\mathbf{n}_i - \mathbf{n}\cdot\mathbf{n}_i(\mathbf{n}_{i-1}\cdot\mathbf{n}_i + \mathbf{n}_i\cdot\mathbf{n}_{i+1})\} - \frac{\beta h^2}{4s}\sum_{i=1}^{N/2}\{\omega[1-(\mathbf{n}\cdot\mathbf{n}_{2i-1})^2] + 1 - (\mathbf{n}\cdot\mathbf{n}_{2i})^2\},$$

$$\mathcal{H}_h^{(2)} = \frac{-\beta^2h^3}{12s^2}\Psi_1 + \frac{\beta^2\omega h^2\tilde{J}}{4s^2}\Psi_2 - \frac{\beta^2\omega h\tilde{J}^2}{4s^2}\Psi_3 - \frac{\beta^2\omega^2\tilde{J}^2h}{4s^2}\Psi_4 - \frac{\beta^2\omega h\tilde{J}^2}{24s^3}\Psi_5. \quad (5)$$

where Ψ_i is expressed in terms of the classical vectors $\mathbf{n}$ and $\mathbf{n}_i$ (see the Appendix). The partition function is represented by the effective Hamiltonian defined in the previous equations,

$$\mathcal{Z}=\left(\frac{2\omega s+1}{4\pi}\right)^{N/2}\left(\frac{2s+1}{4\pi}\right)^{N/2}\int \Pi_{i=1}^{N} d\mathbf{n}_i e^{-\beta\mathcal{H}^{(0)}} \times\left\{\left(1-\beta\mathcal{H}_h^{(0)}+\frac{\beta^2}{2}[\mathcal{H}_h^{(0)}]^2+\cdots\right)\times\left[1-\beta\mathcal{H}_h^{(1)}+\frac{\beta^2}{2}(\mathcal{H}_h^{(1)})^2-\beta\mathcal{H}^{(1)}+\beta^2\mathcal{H}_h^{(1)}\mathcal{H}^{(1)}+\frac{\beta^2}{2}(\mathcal{H}^{(1)})^2-\beta(\mathcal{H}^{(2)}+\mathcal{H}_h^{(2)})+O(1/s^3)\right]\right\}. \quad (6)$$

The reduced magnetic susceptibility is obtained by two times differentiating from the logarithm of the partition function with respect to h, i.e.,

$$\chi=\lim_{H\to 0}\frac{\partial m}{\partial h}. \quad (7)$$

where H is the magnetic field and m is the scaled magnetization per site and given by

$$m=\frac{1}{N}\frac{\partial \ln \mathcal{Z}}{\partial(\beta h)}. \quad (8)$$

In the limit of $H\to 0$, all of the terms containing h^3 or higher orders of h will vanish in the partition function. So, we will keep the expansion up to the second order of h in the partition function Eq. (6). By the integration on the coherent states, we find the scaled magnetization in terms of the coupling and the magnetic field. The reduced magnetic susceptibility is as follow:

$$\chi=\frac{2\beta\omega}{3}\left(\frac{B}{1-B^2}\right)+\frac{\beta(1+\omega^2)}{6}\left(\frac{1+B^2}{1-B^2}\right)+\frac{\beta(\omega+1)}{6s}-\frac{2\beta(1+\omega)}{3s}\left(\frac{B}{1-B}\right)-\frac{\beta^2\tilde{J}\omega}{3s^2}\left(1-B-\frac{B}{\omega\xi}\right), \quad (9)$$

where $\xi=\beta\tilde{J}$ and $B=\coth(\omega\xi)-1/\omega\xi$ is the Langevin function.

We have plotted in Fig. 3 the actual magnetic susceptibility (χ_a) of the ($S=5/2$, $s=2$) ferrimagnetic chain versus temperature. It is related to the susceptibility defined in Eq. (7) by the following relation,

$$\chi_a=\lim_{H\to 0}\frac{\partial m_a}{\partial H}=s^2\chi, \quad (10)$$

where $m_a=sm$ is the actual magnetization. The presented CE result contains the quantum corrections up to the second order of $(\beta\tilde{J}/s)$. We will discuss the quality of our results in comparison with other results in the next section.

B. Quantum Monte Carlo simulation

We have implemented the quantum Monte Carlo (QMC) simulation for the ferrimagnetic ($S=5/2$, $s=2$) chain of length $N=64$. The fairly large attainable length size gives us the thermodynamic properties as a very good approximate of the infinite size chain. In doing so, we have considered the Hamiltonian of Eq. (2) for $N=64$ and without the magnetic field. We utilized the QMC algorithm based on the Suzuki-Trotter decomposition[23] of the checkerboard type.[24] In this respect, we begin by breaking the Hamiltonian into four pieces, $\hat{H}=\hat{H}_0/2+\hat{H}_a+\hat{H}_0/2+\hat{H}_b$, where $\hat{H}_0$ contains the interactions in z direction. $\hat{H}_a$ and $\hat{H}_b$ represent the interaction in the transverse direction alternatively. The partition function is expressed by the Suzuki-Trotter formula as follows:

$$\mathcal{Z}=\mathrm{Tr}\, e^{-\beta\hat{H}}=\lim_{m\to\infty}\mathcal{Z}_m,$$

$$\mathcal{Z}_m:=\mathrm{Tr}(e^{-\beta\hat{H}_0/2m}e^{-\beta\hat{H}_a/m}e^{-\beta\hat{H}_0/2m}e^{-\beta\hat{H}_b/m})^m, \quad (11)$$

where m is a Trotter number. Performing the trace operation, we have a two-dimensional classical Hamiltonian rather than the one-dimensional quantum Hamiltonian. This classical Hamiltonian has $2mN$ spins. We have considered the plaquette flip for the evolution of the Monte Carlo simulation. The reason is related to the huge number of single spin flips which are not permitted because their Boltzmann weight is zero. For instance, in the case of a plaquette of four spins which contains two $S=5/2$ and two $s=2$, there exist 900 different configurations. There are only 110 configurations with nonzero Boltzmann weights. All of these nonzero cases can be obtained by a plaquette flip.[15] The quantities such as internal energy, heat capacity, and magnetic susceptibility depend on the Trotter number (m). In the limit of $m\to\infty$, these quantities tend to their correct values. Therefore, the QMC should take the biggest possible value of m, especially at low temperatures. However, when temperature decreases the convergence relative to m becomes small. In other words, using a big value for m makes two kinds of problems. Firstly, β/m becomes small so the state of the system (spin configuration) changes hardly (evolves slowly). Secondly, when m is large the global flips to change the total magnetization are hard to accept at low temperatures. Consequently, many Monte Carlo steps are needed to equilibrate the system at a large m and low temperature. Therefore, for the mentioned reasons we have performed the calculations for each temperature with different values of m and utilizing the least-square extrapolation method [Eq. (12) to find the limit of $m\to\infty$],

$$A(m)=A_\infty+\frac{A_1}{m^2}+\frac{A_2}{m^4}+\cdots. \quad (12)$$

For moderate and low temperature regimes ($T<3J$) we have considered three different values for the Trotter number, $m=15,20,30$. At higher temperatures, the convergence happens for the lower m values. To equlibriate the system we have spent 10^5 Monte Carlo steps and 10^6 steps for measurement. Accuracy of the measured quantities depends on the temperature; for higher temperatures, we got higher accuracy. However, the error bar is less than the symbol sizes in our plots.

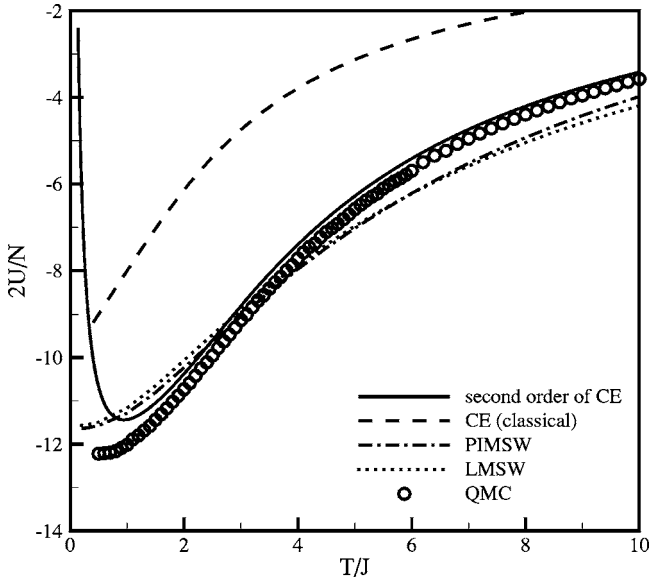

FIG. 1. Temperature dependence of the internal energy per cell of the ferrimagnetic ($S=5/2$, $s=2$) chain. The solid line: cumulant expansion up to the second order; dashed line: classical part of the cumulant expansion; dashed-dotted line: perturbational interacting modified spin-wave theory (PIMSWT); dotted line: linear modified spin-wave theory (LMSWT); and circles: quantum Monte Carlo simulation with $N=64$ spins.

The internal energy, specific heat, and magnetic susceptibility of the ferrimagnetic ($S=5/2$, $s=2$) chain have been plotted in Figs. 1–3 respectively. We will discuss our results in the next section when we compare our results with those of others.

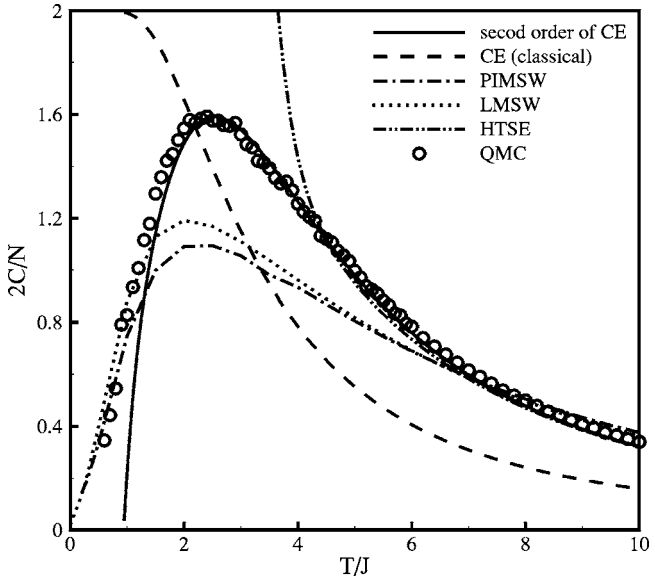

FIG. 2. The specific heat per cell of the ferrimagnetic ($S=5/2$, $s=2$) chain. Cumulant expansion up to second order (solid line), classical part of the cumulant expansion (dashed line), perturbational interacting modified spin-wave theory (dashed-dotted line), linear modified spin-wave theory (dotted line), high temperature series expansion (dashed-dotted-dotted line) and quantum Monte Carlo simulation (open circles) with $N=64$ spins.

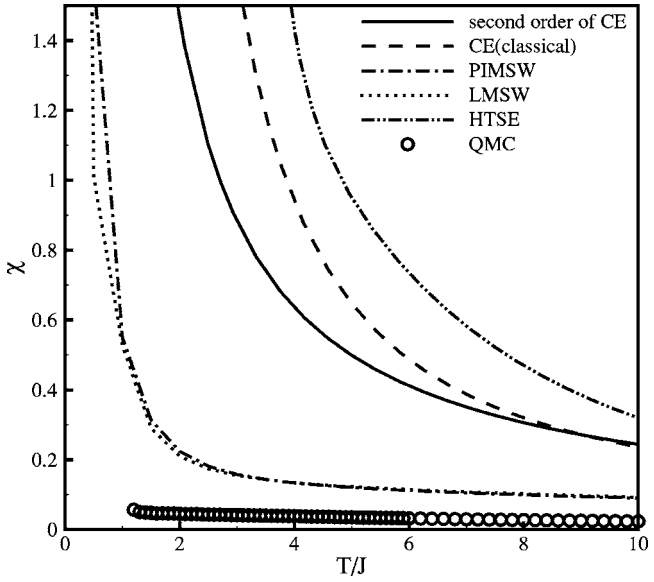

FIG. 3. Magnetic susceptibility per spin of the ferrimagnetic ($S=5/2$, $s=2$) chain versus temperature. The solid line: cumulant expansion up to second order; dashed line: classical part of the cumulant expansion, dashed-dotted line: perturbational interacting modified spin-wave theory (PIMSWT); dotted line: linear modified spin-wave theory (LMSWT); dashed-dotted-dotted line: High temperature series expansion; and circles: quantum Monte Carlo simulation with $N=64$ spins.

C. Modified spin-wave theory

In the modified spin-wave theory, usually it is considered a single-component bosonic representation of each spin variable at the cost of the rotational symmetry. To simplify in the incoming calculations, we consider the following form of the Hamiltonian for the ferrimagnetic chain:

$$\hat{H} = J\sum_{i=1}^{N} (\mathbf{S}_i \cdot \mathbf{s}_{i-1} + \mathbf{s}_i \cdot \mathbf{S}_i). \tag{13}$$

Using the Holestain-Primakoff and the Bogoliubov transformation, the Hamiltonian (13) is diagonalized $\mathcal{H}=-2NJSs+E_1+E_0+\mathcal{H}_1+\mathcal{H}_0+O(S^{-1})$, where E_i gives the $O(S^i)$ quantum corrections to the ground state energy and $\mathcal{H}_i$ is expressed in terms of $\alpha_k^\dagger$ and $\beta_k^\dagger$ and gives the quantum corrections to the dispersion relation (see Ref. 13). $\alpha_k^\dagger$ and $\beta_k^\dagger$ are the creation operators of the ferromagnetic and antiferromagnetic spin waves with momentum k, respectively.

At finite temperatures, we assume that $\tilde{n}_k^{\pm} \equiv \Sigma_{n^-,n^+} n^{\pm} P_k(n^-,n^+)$ for the spin-wave distribution functions, where $P_k(n^-,n^+)$ is the probability of n^- ferromagnetic and n^+ antiferromagnetic spin waves appearing in the k-momentum state and satisfies $\Sigma_{n^-,n^+} P_k(n^-,n^+)=1$ for all k's.[13] The substitutions $\tilde{n}_k^- = \alpha_k^\dagger \alpha_k$ and $\tilde{n}_k^+ = \beta_k^\dagger \beta_k$ in the spin-wave Hamiltonian gives the zero-field free energy,

$$F = E_g + \sum_k (\tilde{n}_k^- \omega_k^- + \tilde{n}_k^+ \omega_k^+) + T\sum_k \sum_{n^-,n^+} P_k(n^-,n^+) \ln P_k(n^-,n^+). \tag{14}$$

To keep the number of bosons finite, one should apply the following constraint,

$$\langle :S^z - s^z: \rangle = (S+s)N - (S+s)\sum_k \sum_{\sigma=\pm} \frac{\tilde{n}_k^\sigma}{\omega_k} = 0, \qquad (15)$$

where $\omega_k = [(S-s)^2 + 4Ss\sin^2 k]^{1/2}$ and the normal ordering is taken with respect to α and β. By minimization of the free energy (14) with respect to $P_k(n^-, n^+)$'s under the condition (15) we can obtain the free energy and the magnetic susceptibility at thermal equilibrium as follows:

$$F = E_g + \mu(S+s)N - T\sum_k \sum_{\sigma=\pm} \ln(1+\tilde{n}_k^\sigma), \qquad (16)$$

$$\chi = \frac{1}{3T}\sum_k \sum_{\sigma=\pm} \tilde{n}_k^\sigma (1+\tilde{n}_k^\sigma), \qquad (17)$$

where $\tilde{n}_k^\pm = [e^{[J\omega_k^\pm - \mu(S+s)/\omega_k]/T} - 1]^{-1}$, and μ is the Lagrange multiplier to consider the constraint (15). This set of equations has no closed analytic solution. In the case of ($S=5/2$, $s=2$) we have numerically solved Eqs. (15) and (16) in the thermodynamic limit, and visualized them in Figs. 1–3. In previous equations we have chosen $k_B=1$. ω_k^- and ω_k^+ are the ferromagnetic and antiferromagnetic excitation gaps, respectively. They have different values in the linear modified spin-wave theory (LMSWT) and perturbational interacting modified spin-wave theory (PIMSWT). In the PIMSWT, the $O(S^0)$ terms have been considered. Because the antiferromagnetic excitation gap is significantly improved by the inclusion of the $O(S^0)$ correlation, the location of the Schottky peak can be also reproduced very well by the perturbational interacting modified spin waves.

III. RESULTS AND DISCUSSIONS

We have obtained the effective Hamiltonian of the ferrimagnetic chains in the presence of an external magnetic field to second order of cumulant expansion, Eq. (5). The zeroth order term shows the classical contribution which simply represents the coupling energy of the classical spins with the external magnetic field. Quantum corrections have a non-Heisenberg form and they are important in the intermediate temperatures.

In Fig. 1, we have shown the internal energy per unit cell of spins ($2U/N$) versus temperature. The big difference between the zeroth order (classical contribution shown by dashed line) and the second order cumulant expansion (quantum corrections shown by solid line) shows the importance of the corrections in the intermediate and higher temperatures. The discrepancy is high, even in the present case of fairly large spins ($S=5/2$, $s=2$) which seems to behave classically. The reason is related to the dual features of ferrimagnets, i.e., the low temperature behavior is like ferromagnets and the high temperature behavior like antiferromagnets. There is a spectral gap in the subspace $S_{tot}=N/2(S-s)+1$, where the optical magnons play an important role. In the case of ($S=5/2$, $s=2$), the spectral gap of optical magnons at $k=0$ is $\Delta_0=1.36847J$ (Ref. 25). This means that the model does not behave purely classically. So, to describe the finite temperature behavior of the system, we should consider the quantum corrections to the classical part. At low temperature the second order of CE has a large deviation in comparison with the other results, because in the low temperature region classical fluctuations are not strong enough to suppress the quantum ones. However, the low temperature region has been excluded from the convergence domain by construction when CE is expressed as a series in the order of $\beta Js < 1$. Obviously, the classical term is dominant at very high temperatures.

To have an impression on the accuracy of our results, we have plotted the results of the QMC simulation for comparison. The second order CE of the internal energy in Fig. 1 fits very well on the QMC results for $T > 2J$. This is actually the validity regime of our CE approach, $T > Js$. We have also plotted in Fig. 1 the results of two different modified spin-wave theories which deviate slightly from the QMC ones. However, the accuracy of the different schemes can be best visualized in the physical quantities such as the specific heat and the magnetic susceptibility, which are shown in Figs. 2 and 3.

In Fig. 2, we have plotted the specific heat per unit cell of spins ($2C/N$) for a ($S=5/2$, $s=2$) ferrimagnetic chain. The results of CE have been shown as the pure classical contribution and also the whole contribution to the second order. The big difference between them verifies the significant corrections of the second order CE. We have also plotted the result of QMC simulation, for comparison. We observe very good agreement between the CE and the QMC results. According to the results presented in Figs. 1 and 2, the QMC simulation results confirm that the CE is a very good analytical approach to describe the thermodynamic properties of a ferrimagnetic system with large spins at moderate and high temperatures.

We have also shown in Fig. 2 the results of the MSWT for the specific heat. We have examined the LMSW and the PIMSW for our system. As observed from Fig. 2, both the LMSW and PIMSW can reproduce the high temperature behavior of heat capacity close to the QMC simulation results. Furthermore, they can show the Schottky peak at midtemperatures. Although the PIMSW can reproduce the location of the Schottky peak fairly well, it cannot estimate the peak value well for large spins in comparison with the CE. The reason of this discrepancy in the MSWT is as follows. Let us come back to the spin-wave theory and draw your attention to the bosonic Hamiltonian, $\mathcal{H} = -2NJSs + E_1 + E_0 + \mathcal{H}_1 + \mathcal{H}_0 + O(S^{-1})$ where

$$\mathcal{H}_i = J\sum_k [\omega_i^-(k)\alpha_k^\dagger\alpha_k + \omega_i^+(k)\beta_k^\dagger\beta_k + \gamma_i(k)(\alpha_k\beta_k + \alpha_k^\dagger\beta_k^\dagger)], \qquad (18)$$

and $\gamma_i(k)$'s have been introduced in Ref. 13. The last two terms in $\mathcal{H}_i$ are the normal-ordered quasiparticle interactions. In MSWT, whether LMSW or PIMSW, we have eliminated these interactions, i.e., we choose

$$\gamma_1(k) = 0 \rightarrow \tanh 2\theta_k = \frac{2\sqrt{Ss}\cos k}{S+s}.$$

However, in the low and moderate temperatures, the magnon-magnon interactions play an important role. There-

fore it is surmised that if we consider at least the first order of the quasiparticle interaction [i.e., $\gamma_1(k) \neq 0$ and $\gamma_0(k)=0$], we can produce the Schottky peak value more precisely. Although the agreement between MSWT (without the quassiparticle interaction) and the other results is not perfect, it is a remarkable success for the spin-wave theory in the one-dimensional large spin ferrimagnet that all relevant features are quantitatively rather well reproduced over a very large temperature range.

Finally, we have plotted in Fig. 3 the magnetic susceptibility per total number of spins (χ/N) of the ($S=5/2$, $s=2$) ferrimagnetic chain versus temperature. The result of the second order CE is shown by the solid line. The CE result shows qualitatively the features of the ferrimagnetic chains, i.e., the quasiclassical χ shows the divergence for $T \to 0$ like a ferromagnet and a Curie law ($1/T$) decay at high temperatures. Meanwhile in Fig. 3 we have plotted the result of the QMC simulation. Our simulation result shows very well the antiferromagnetic feature of the ferrimagnetic system, but it cannot produce the ferromagnetic behavior at low temperatures. The reason is as follows. The antiferromagnetic trait of the model does not depend on the size of system, i.e., all antiferromagnetic features can be reproduced in a rather short system size, while the ferromagnetic ones completely depend on the number of spins. This means that the ferromagnetic features emerge only slowly with the growing of system size. In the QMC approach we have considered 32 cells (64 spins) for simulation. The computation time grows exponentially by going to larger sizes, and especially happens in the calculation of magnetic susceptibility to reach the equilibrium condition. However, our main interests in this study are the results for intermediate and large temperature regions where reasonable values exist.

We have also shown in Figs. 2 and 3 the results of HTSE for the specific heat and the susceptibility of ($S=5/2$, $s=2$) ferrimagnetic chain, respectively. The HTSE is an expansion in powers of βJ. Recently, Fukushima and his collaborators have implemented a suitable Padé approximation to obtain the thermodynamic functions of the mixed spin chains. They have found the specific heat and the susceptibility up to $[O(\beta J)^{11}]$ and $[O(\beta)^7]$, respectivly.[14] The HTSE results for the specific heat shown in Fig. 2 converges to the QMC results at $T>4J$. However, the deviation from the QMC result is more pronounced for the magnetic susceptibility shown in Fig. 3.

It is worth mentioning the two differences between the CE and HTSE results. Firstly, the convergence region of CE is larger than the HTSE one, i.e., the CE is valid for $T>Js$ whereas the validity of the HTSE is for $T>\sqrt{S(S+1)}J$. Secondly, the HTSE fails to produce the Schottky peak of the specific heat, while the CE can generate it as well as the QMC simulation.

Our results state that the combined methods of the cumulant expansion for $T>Js$ and the modified spin-wave theory for $T<Js$, give a good approximation for the whole finite temperature behavior of quantum ferrimagnets. The reason is related to the overlap of the convergence regions of the mentioned method.

ACKNOWLEDGMENT

A. L. would like to acknowledge the hospitality of the Max-Planck-Institut für Chemische Physik fester Stoffe in Dresden where the final preparation of this work was done.

APPENDIX

The expressions of the second term ($\mathcal{H}_h^{(2)}$) of the field-dependent effective Hamiltonian are obtained as follows,

$$\Psi_1 = \sum_{i=1}^{N/2} \{\omega \mathbf{n}\cdot\mathbf{n}_{2i-1}[1-(\mathbf{n}\cdot\mathbf{n}_{2i-1})^2] + \mathbf{n}\cdot\mathbf{n}_{2i}[1-(\mathbf{n}\cdot\mathbf{n}_{2i})^2]\},$$

$$\Psi_2 = \sum_{i=1}^{N} \{1-2(\mathbf{n}\cdot\mathbf{n}_i)^2 + (\mathbf{n}\cdot\mathbf{n}_i)(\mathbf{n}_i\cdot\mathbf{n}_{i+1})(\mathbf{n}_{i+1}\cdot\mathbf{n}) - \mathbf{n}_i\cdot\mathbf{n}_{i+1} - (\mathbf{n}\cdot\mathbf{n}_i)(\mathbf{n}\cdot\mathbf{n}_{i+1}) + (\mathbf{n}_i\cdot\mathbf{n}_{i+1}) \times [(\mathbf{n}\cdot\mathbf{n}_i)^2 + (\mathbf{n}\cdot\mathbf{n}_{i+1})^2]\},$$

$$\Psi_3 = \sum_{i=1}^{N} (\mathbf{n}\cdot\mathbf{n}_i)\{(\mathbf{n}_{i-1}\cdot\mathbf{n}_i)^2 + (\mathbf{n}_i\cdot\mathbf{n}_{i+1})^2\} + \sum_{i=1}^{N/2} \{2(\mathbf{n}\cdot\mathbf{n}_{2i-1}) \times (\mathbf{n}_{2i-1}\cdot\mathbf{n}_{2i})(\mathbf{n}_{2i-1}\cdot\mathbf{n}_{2i-2}) + (\mathbf{n}\cdot\mathbf{n}_{2i})(\mathbf{n}_{2i}\cdot\mathbf{n}_{2i-1}) \times (\mathbf{n}_{2i-1}\cdot\mathbf{n}_{2i-2}) + (\mathbf{n}\cdot\mathbf{n}_{2i-2})(\mathbf{n}_{2i-2}\cdot\mathbf{n}_{2i-1})(\mathbf{n}_{2i-1}\cdot\mathbf{n}_{2i}) - (\mathbf{n}\cdot\mathbf{n}_{2i-2} + \mathbf{n}\cdot\mathbf{n}_{2i-1} + \mathbf{n}\cdot\mathbf{n}_{2i}) \times + (\mathbf{n}\cdot\mathbf{n}_{2i-2}) \times (\mathbf{n}_{2i-2}\cdot\mathbf{n}_{2i-1})(\mathbf{n}_{2i-1}\cdot\mathbf{n}_{2i}) - (\mathbf{n}\cdot\mathbf{n}_{2i-2} + \mathbf{n}\cdot\mathbf{n}_{2i-1} + \mathbf{n}\cdot\mathbf{n}_{2i}) \times (\mathbf{n}_{2i-1}\cdot\mathbf{n}_{2i} + \mathbf{n}_{2i-2}\cdot\mathbf{n}_{2i-1}) - (\mathbf{n}_{2i}\cdot\mathbf{n}_{2i-2}) \times (\mathbf{n}\cdot\mathbf{n}_{2i} + \mathbf{n}\cdot\mathbf{n}_{2i-2})\}$$

$$\Psi_4 = \sum_{i=1}^{N} (\mathbf{n}\cdot\mathbf{n}_i)[(\mathbf{n}_{i-1}\cdot\mathbf{n}_i)^2 + (\mathbf{n}_i\cdot\mathbf{n}_{i+1})^2] + \sum_{i=1}^{N/2} \{2(\mathbf{n}\cdot\mathbf{n}_{2i}) \times (\mathbf{n}_{2i}\cdot\mathbf{n}_{2i-1})(\mathbf{n}_{2i}\cdot\mathbf{n}_{2i+1}) + (\mathbf{n}\cdot\mathbf{n}_{2i-1})(\mathbf{n}_{2i-1}\cdot\mathbf{n}_{2i}) \times (\mathbf{n}_{2i}\cdot\mathbf{n}_{2i+1}) + (\mathbf{n}\cdot\mathbf{n}_{2i+1})(\mathbf{n}_{2i+1}\cdot\mathbf{n}_{2i})(\mathbf{n}_{2i-1}\cdot\mathbf{n}_{2i}) - (\mathbf{n}\cdot\mathbf{n}_{2i-1} + \mathbf{n}\cdot\mathbf{n}_{2i+1} + \mathbf{n}\cdot\mathbf{n}_{2i}) \times (\mathbf{n}_{2i-1}\cdot\mathbf{n}_{2i} + \mathbf{n}_{2i}\cdot\mathbf{n}_{2i+1}) - (\mathbf{n}_{2i-1}\cdot\mathbf{n}_{2i+1})(\mathbf{n}\cdot\mathbf{n}_{2i-1} + \mathbf{n}\cdot\mathbf{n}_{2i+1})\}$$

$$\Psi_5 = \sum_{i=1}^{N/2} \{(1-\mathbf{n}_{2i-1}\cdot\mathbf{n}_{2i})[2\mathbf{n}\cdot\mathbf{n}_{2i} + 2\mathbf{n}\cdot\mathbf{n}_{2i-1} + (1 - 3\mathbf{n}_{2i-1}\cdot\mathbf{n}_{2i})(\mathbf{n}\cdot\mathbf{n}_{2i-1} + \mathbf{n}\cdot\mathbf{n}_{2i})] + (1-\mathbf{n}_{2i-1}\cdot\mathbf{n}_{2i-2}) \times [2\mathbf{n}\cdot\mathbf{n}_{2i-2} + 2\mathbf{n}\cdot\mathbf{n}_{2i-1} + (1 - 3\mathbf{n}_{2i-1}\cdot\mathbf{n}_{2i-2})(\mathbf{n}\cdot\mathbf{n}_{2i-1} + \mathbf{n}\cdot\mathbf{n}_{2i-2})]\}$$

[1] S. Blundell, *Magnetism in Condensed Matter* (Oxford University Press, New York, 2001); O. Kahn, *Molecular Magnets* (VCH, New York, 1993) and references therein.
[2] M. Abolfath, H. Hamidian, and A. Langari, cond-mat/9901063 (and references therein), Phys. Rev. B (to be published).
[3] M. Verdaguer, A. Gleizes, J. P. Renard, and J. Selden, Phys. Rev. B **29**, 5144 (1984); M. Hagiwara, J. Phys. Soc. Jpn. **67**, 2209 (1998); Y. Hosokoshi, Y. Nakazawa, K. Indue, K. Takizawa, H. Nakano, M. Takahashi, and M. Goto, Phys. Rev. B **60**, 12924 (1999).
[4] F. D. M. Haldane, Phys. Rev. Lett. **50**, 1153 (1983); Phys. Lett. **93A**, 464 (1983).
[5] A. K. Kolezhuk, H.-J. Mikeska, and S. Yamamoto, Phys. Rev. B **55**, R3336 (1997); S. Brehmer, H.-J. Mikeska, and S. Yamamoto, J. Phys.: Condens. Matter **9**, 3921 (1997); S. K. Pati, S. Ramasesha, and D. Sen, Phys. Rev. B **55**, 8894 (1997); J. Phys.: Condens. Matter **9**, 8707 (1997); S. Yamamoto, T. Fukui, K. Maisinger, and U. Schollwock, *ibid.* **10**, 11033 (1998).
[6] S. Yamamoto and T. Fukui, Phys. Rev. B **57**, R14008 (1998).
[7] S. Yamamoto, S. Brehmer, and H.-J. Mikeska, Phys. Rev. B **57**, 13610 (1998).
[8] S. Yamamoto and T. Sakai, Phys. Rev. B **62**, 3795 (2000).
[9] S. Yamamoto, Phys. Rev. B **59**, 1024 (1999).
[10] M. Abolfath and A. Langari, Phys. Rev. B **63**, 144414 (2001).
[11] T. Sakai and S. Yamamoto, Phys. Rev. B **60**, 4053 (1999).
[12] S. Yamamoto and T. Sakai, J. Phys.: Condens. Matter **11**, 5175 (1999).
[13] S. Yamamoto, Phys. Rev. B **69**, 064426 (2004).
[14] N. Fukushima, A. Honecher, S. Wessil, and W. Brenig, Phys. Rev. B **69**, 174430 (2004).
[15] A. Ghasemi, M.Sc. thesis, Institute for Advanced Studies in Basic Sciences, Zanjan, 2004.
[16] P. Fulde, *Electron Correlations in Molecules and Solids* (Springer, Berlin, 1995).
[17] K. Kladko and P. Fulde, Int. J. Quantum Chem. **66**, 377 (1998).
[18] K. Kladko, P. Fulde, and D. A. Garanin, Europhys. Lett. **46**, 425 (1999).
[19] D. A. Garanin, K. Kladko, and P. Fulde, Eur. Phys. J. B **14**, 293 (2000).
[20] J. Abouie and A. Langari, Phys. Rev. B **70**, 184416 (2004).
[21] J. Abouie and A. Langari, J. Phys.: Condens. Matter **17**, S1293 (2005).
[22] A. Auerbach, *Interacting Electrons and Quantum Magnetism* (Springer, Berlin, 1994).
[23] M. Suzuki, Prog. Theor. Phys. **56**, 1454 (1976).
[24] J. E. Hirsch, R. L. Sugar, D. J. Scalapino, and R. Blankenbecler, Phys. Rev. B **26**, 5033 (1982).
[25] S. Yamamoto, T. Fukui, and T. Sakai, Eur. Phys. J. B **15**, 211 (2000).